SDC Internal Report 96-01

Summary of Initial Work on Ammonium Perchlorate (AP)

Michael Winey

August 1996

Shock Dynamics Center
Washington State University
Pullman, WA 99164-2814

This report summarizes our spectroscopy work on ammonium perchlorate (AP) up to July, 1996. The long range objective of the AP work is to observe and characterize shock-induced decomposition in single-crystal samples. The goal of this present work was to establish workable methods for performing both absorption and Raman experiments on single-crystal AP samples and to draw some initial conclusions from these data about the response of AP to shock loading.

In Section I, some of the properties of AP are listed. Handling considerations and the preparation of samples for experiments are then discussed in Section II. Section III describes the equation of state which we are currently using, while the configurations and results of the spectroscopy experiments are presented in Section IV. A discussion of the experimental results is given in Section V, and the conclusions, along with suggestions for future work, are summarized in Section VI.

I. Physical Properties of AP

A list of selected physical properties of AP is given in Table 1. AP has an orthorhombic crystal structure with the space group Pnma, with 4 molecules in the unit cell[5]. AP is a soft crystal which cleaves easily along the (210), (001), and $(\bar{2}10)$ planes[6]. However, there are really just two distinct cleavage planes, since the (210) plane and the $(\bar{2}10)$ plane are crystallographically equivalent. The different cuts are easily distinguished since crystals cleaved along the (210) and $(\bar{2}10)$ planes have square cleavage faces, whereas the (001) face is shaped like a rhombus.

A melting temperature of 723 K has been reported for AP[7]; however, decomposition and sublimation generally begin before the melting temperature is reached[3]. Decomposition temperatures as low as 475 K have been reported[8], but no time scales for the decomposition were given. A high temperature solid-solid phase transition has been observed at 513 K, which involves an change from the orthorhombic lattice to a cubic structure[3].

II. Handling and Preparing AP Samples

In working with AP crystals, there are several handling considerations to be aware of. First, AP is hygroscopic[7], therefore it should be stored in a desiccator. Skin oil will etch AP, therefore gloves or finger cots should be worn when handling the crystals. AP is also soluble in many polar solvents. In particular, contact with water, acetone, and alcohols should be avoided. AP has been tested and found to be insoluble in the following common solvents: benzene, toluene, hexane, CCl_4, heptane, and hexene. AP is also insoluble in methylene chloride; however, test samples showed cracking due to thermal stresses caused by evaporative cooling from the solvent.

Should it be necessary, AP can be cleaved with a good razor blade. A sharp tap on the razor blade with a makeshift hammer is usually sufficient to produce the cleavage. Experience has shown that the results of a cleavage operation become more unpredictable for larger surface areas of the intended cleavage face. In particular, attempts to reduce the thickness of large sample pieces by cleaving have not been successful.

Sample preparation has been found to proceed well using the following prescription: Rough grinding is done on adhesive-backed 600 grit sandpaper attached to lapped steel surface. The grinding is done wet, using a saturated solution of AP in water to wet the surface. Distilled water can be added to the solution to increase the rate of material removal. Distilled water can also be used to clean the paper when it loads up with AP. Fine grinding is done dry, using 9 micron aluminum oxide lapping sheets (Angstromlap from Fiber Optic Center) on a glass plate. These sheets can be cleaned by rinsing with water, followed by alcohol, although fresh sheets work best. The rough polishing step is accomplished by using 1 micron aluminum oxide powder suspended in oil (Automet Lapping Oil from Buehler). The polishing is done on an adhesive backed cloth (Chemomet cloth from Buehler) attached to a glass plate. Contamination is controlled by rinsing the cloth occasionally with oil. The final polish is produced using the same polishing procedure, but with .3 micron aluminum oxide powder. All grinding and polishing is done under the laminar-flow clean hood.

During the grinding and polishing process, the sample flatness is checked periodically on an optical flat. Sample flatness is most easily produced at the fine grinding stage. The polishing stages tend to produce curvature of the sample surface. Therefore, the amount of polishing is kept to a minimum.

III. Equation of State for AP

Pressures and temperatures for shocked AP are currently calculated using a very simple equation of state (EOS). As implemented in the SHOCKUP code, the specific heat and the Gruneisen ratio, Γ/v, are both held constant, using values (1.26 J/g-K and 1.45, respectively) taken from Sandstrom, et al.[4]. The reference curve used is the Hugoniot derived by G. Yuan from his continuum measurements of shocked AP[2] ($U_s = 2.725 + 2.190\ u_p$) The 5 kbar Hugoniot elastic limit of AP has been ignored here, so the Hugoniot for the plastic wave has been used. The implementation of the EOS in the COPS code is similar, except that the AP has been modeled as an elastic-perfectly plastic material. Thus, the 5 kbar elastic precursor has been explicitly accounted for. A sample input file for the COPS code is provided in Appendix A.

IV. Spectroscopy Experiments

Both absorption and Raman experiments were carried out on (210)-oriented AP. The experimental parameters from these experiments are listed in Table 2. The experimental configurations are discussed below, pointing out both successful and unsuccessful methods of sample preparation and cell construction. Results from each experiment are then presented and the important features are pointed out.

A. Absorption Experiments. The absorption spectrum of AP could not be found in the literature, so an ambient spectrum was acquired on the UV/VIS absorption spectrometer in the WSU Chemistry Department. This spectrum showed no absorption features for wavelengths longer than 210 nm. Below 210 nm, the transmission dropped rapidly, but it was not clear if this absorption was due to the AP or due to impurities.

1. *Experimental Configuration.* Two different experimental configurations were used in the absorption experiments. The first configuration, used in Experiment 1, was a thick sample configuration where the AP sample was impacted directly by the sapphire impactor. The transmission of light through the cell was then measured as the initial shock traversed the sample.

The second configuration, used in Experiment 2, was a thin sample configuration. As shown in Figure 1, the sample was contained between LiF windows. These crystals were bonded together with the Epo-Tek 305 UV-transmitting epoxy, which was transparent over the 270 - 550 nm range of the absorption system. The LiF front window was then impacted by a sapphire impactor, as with the liquid cells, resulting in a stepwise loading process in the AP sample. The method of delivery of the flashlamp light to the target and the method of collection of the transmitted light are both identical to the methods used in previous nitromethane experiments[9].

2. *Experimental Results.* In Experiment 1, no new absorption peaks were observed as the shock traversed the sample. However, a broadband attenuation was observed, starting at the time of impact of the sapphire on the AP sample and increasing with time. The increase in attenuation with time was attributed the increase in the amount of shocked sample as the shock wave swept through the AP. Analysis of these results were hindered by the lack of spatial resolution in the thick samples. Therefore, thick sample absorption experiments were discontinued.

In Experiment 2, a thin sample was used so that adequate spatial resolution could be obtained and absorption results could be more reliably interpreted. Figure 2 shows the time-resolved absorption spectra from this experiment. As the shock enters the sample, a broadband increase in attenuation is observed. This attenuation is not spectrally flat, but is stronger at shorter

wavelengths. This seems to indicate that the attenuation is due to the tail of some absorption peak farther into the UV. Once again it is not clear if this is AP absorption or some impurity band. After peak pressure is reached in the sample, no further spectral changes were observed. Thus, no signs of chemical reaction were observed in this experiment.

B. Raman Experiments. The Raman spectrum of AP can be found in the literature, where reliable peak assignments have been previously made[8]. The observed peaks are thus identified as the ClO_4^- bending mode (E symmetry) at 461 cm^{-1}, the ClO_4^- bending mode (T_2 symmetry) at 627 cm^{-1}, the ClO_4^- symmetric stretching mode (A_1 symmetry) at 933 cm^{-1}, the ClO_4^- antisymmetric stretching mode (T_2 symmetry) at about 1100 cm^{-1}, and the NH_4^+ symmetric stretching mode (A_1 symmetry) at 3204 cm^{-1}. There is also an NH_4^+ antisymmetric stretching mode (T_2 symmetry) at 3350 cm^{-1} and NH_4^+ bending modes at 1420 cm^{-1} (E symmetry) and at 1680 cm^{-1} (T_2 symmetry). However, these modes are weak and are not resolvable in our spectra.

1. *Experimental Configuration.* The three Raman experiments were each done in a different configuration. To avoid focusing the laser on an epoxy bond, Experiment 3 was performed in the thick sample configuration. The sample was sufficiently thick that the laser could be easily focused in the middle, away from either surface. To achieve a reasonable spatial resolution, the laser light was incident on the LiF back window at an angle of 60 degrees from the surface normal and the signal collection was done at an angle of 30 degrees, so that there was a 90 degree angle between them. This produced an overlap of the two focal regions which had a reasonably small dimension perpendicular to the shock front. The transit time of the shock wave through this region was calculated to be about 200 ns, which was the effective time resolution for this experiment. However, as discussed later, this configuration suffered from serious elastic scattering problems.

To obtain better time resolution and to reduce the elastic scattering, Experiment 4 was performed in a thin sample configuration with the laser and collection angles at the usual 45 and 0 degrees, respectively. As in Experiment 2, the sample was contained between two LiF windows and the front window was impacted with a sapphire impactor. To avoid laser damage to the sample-window interfaces, the sample was attached to the windows by epoxying around the edges, so that the central region of the interfaces was epoxy-free.

After the results of Experiment 4 proved unsatisfactory, an attempt was made to bond the sample to the windows with epoxy. It was discovered that a bond using the Epo-Tek 305 epoxy could sustain laser energies of over 80 mJ, compared to less than 30 mJ for the Hysol 815 epoxy. However, the Epo-Tek 305 epoxy was found to fluoresce due to reaction with the AP sample. Later tests with the Epo-Tek 301 epoxy produced similar results.

Therefore, in Experiment 5, a thin sample configuration was used which was similar in design to the liquid cell experiments (see Ref. 9). In this configuration, shown in Figure 3, hexane was used to fill the interface between the AP sample and the windows. As in previous liquid cell experiments, a sapphire back window was used. However, the cell design used in this experiment involved a slight modification to the nitromethane cells[9]. To achieve an intimate contact between LiF front window and the AP sample, the LiF window did not rest on a machined surface of the brass cell body. Rather, as shown in Figure 3, the O-ring groove for the LiF front window was cut shallower than usual and the window rested directly on the AP sample. Because the front window rested on the sample, the depth of the O-ring groove had to be carefully calculated, taking into account the position of the sapphire back window and the thickness of the AP sample. The window was pressed against the sample with a set of 8 set screws in the brass retaining ring. Alignment of the window with the sample was achieved by adjusting the set screws while viewing the cell under monochromatic light. Proper alignment was indicated when the interference fringe patterns were roughly centered on the sample. The cell was then filled with hexane as in the liquid cell experiments[9]. One additional change from liquid cell experiments involved the use of Viton O-rings. This was made necessary since hexane caused swelling in the ethylene propylene O-rings used in the nitromethane experiments[9].

2. *Experimental Results.* In Experiment 3, a huge increase in elastic scatter was observed when the shock in the AP sample reached the collection region for the scattered light. All the Raman modes except the NH_4^+ stretching mode were completely swamped out by this extraneous light. The dominant spectral features were the fused silica Raman modes from the optical fibers.

In Experiment 4, the signal quality was good until the shock reached the back of the AP sample. At this point, the background rose rapidly, reaching a maximum just after peak pressure was reached. After this, the background gradually came down over the remainder of the experiment. The observed background rise was attributed to emission from the air gap at the sample-window interface. The Raman peak for the ClO_4^- (A_1) stretch, which was still observable despite the large background, showed the expected pressure-induced shift to higher vibrational energy. However, the low signal to noise ratio prevented farther conclusions from being drawn.

No such background increase was observed in Experiment 5. In fact, after peak pressure was reached, there were no significant spectral changes for the duration of the experiment. Two spectra from this experiment, one prior to the arrival of the shock in the sample and the other after peak pressure was reached, are shown in Figure 4. The pressure-induced hardening of all modes and the lack of a significant background rise are clearly evident. The small shift in position of the ClO_4^- (T_2) bend is noteworthy, as is the broadening of the ClO_4^- E and T_2 bends, relative to the A_1

stretching mode of ClO_4^- and NH_4^+. The antistokes peaks of the E bend and the A_1 stretch of the ClO_4^- ion are also visible after peak pressure is reached.

V. Discussion of Results

Because no absorption peaks were visible in the ambient UV/VIS spectrum of AP, it is hard to extract information from Experiments 1 and 2. The pressure-induced attenuation, shown in Figure 2, extends out to 514 nm. However, given the lack of pressure-induced resonance effects in the Raman spectrum of Figure 4, it is unreasonable to assign the attenuation to absorption in the AP bulk. Rather, it is most likely due to impurity absorptions in the sample. The shape of the absorption profile seems to indicate that the peaks of these impurity bands lie deeper into the UV. Since no significant spectral changes occur after peak pressure is reached, the absorption experiments show no evidence of reaction within our experimental time window for a peak pressure of 11.0 GPa and a temperature of 440 K.

A similar lack of spectral changes after peak pressure is reached in Experiment 5 indicates that reaction is not observed to a peak pressure of 15.8 GPa and a temperature of 446 K. This is in contrast with the results of Sandusky, et al.[6], who reported a shock-induced reaction threshold of 25 kbar based on analysis of recovered samples. The present spectroscopy experiments show that the reaction observed by Sandusky, et al. must have occurred long after the passage of the shock wave, under uncertain loading and thermal conditions.

Despite the lack of evidence for reaction, interesting shock-induced effects are observed in Experiment 5. For instance, it is not clear why the ClO_4^- (T_2) bend shows such a small pressure-induced frequency shift. In addition, the large broadening of the ClO_4^- E and T_2 bending modes is quite interesting. Two potential explanations for this broadening exist at the current time. The first explanation is that the uniaxial strain from the shock causes a lifting of the degeneracy of the E and T_2 modes. This would result in splitting of the Raman lines, as in the work of Boteler and Gupta on shocked diamond[10]. The expected degree of splitting in shocked AP has not been calculated, so the viability of this explanation is not known.

The second explanation involves the possibility of a shock-induced phase transition. It has been observed that the ClO_4^- E and T_2 bending modes exhibit considerable broadening, relative to the other modes, when the orthorhombic-cubic phase transition is reached at atmospheric pressure[8]. This broadening was linked to the possible onset of unhindered rotation of the ClO_4^- tetrahedra in the lattice. These rotations, in turn, were suggested as a destabilizing factor in the AP lattice. A similar phenomenon may be occurring in the present experiments as well. However, the elastic-plastic transition at 5 kbar may also play a role in the observed spectral changes. The effect of plastic deformation on the vibrational properties of AP is not currently known.

VI. Conclusions from Present Work and Suggestions for Future Work

Methods for performing time-resolved absorption and Raman spectroscopy on shocked AP were developed and were demonstrated to be workable. High-quality absorption and Raman spectra for shocked AP have been acquired. Initial results at peak pressures up to 15.8 GPa and temperatures up to 446 K show no evidence for the onset of chemical reaction, in contrast with previous work on recovered samples[6]. Some evidence for possible shock-induced changes in the AP lattice has been observed in the Raman experiments.

These results lead to some suggestions regarding future work. Since the long range objective of the AP project is to observe shock-induced chemical reaction, higher sample pressures and temperatures will have to be reached. Even though decomposition has been observed at 475 K[8], it expected that much higher temperatures will be necessary to observe reaction on the ~ 1 μs time scales of our experiments. It is therefore unlikely that the 4 inch gun can provide adequate projectile velocities for this task. We will therefore need to develop the capability to do Raman experiments on the powder gun.

In planning future experiments, it is necessary to be able to predict the peak pressure and temperature that will be achieved. However, the current equation of state (EOS) contains some simplifying assumptions that are likely to produce erroneous temperature values. Refinements to this EOS are therefore necessary. The observation of antistokes modes in Experiment 5 showed the feasibility of performing stokes/antistokes temperature measurements on shocked AP. Such measurements would be helpful in guiding EOS development.

Because of previous speculations regarding the interpretation of the broadening of the ClO_4^- E and T_2 bending modes[8], it may be worthwhile to do a high resolution experiment to see if any conclusions can be made about the origin of the broadening observed in Experiment 5. Such information may help in understanding the molecular-level changes leading up to reaction.

Acknowledgments

Paul Bellamy is acknowledged for his early contributions to our understanding of the handling and preparation of the AP samples. Dave Savage is acknowledged for developing most of the sample preparation techniques described here. Dr. Thomas Boggs at China Lake is thanked for supplying the AP crystals used in this work.

Appendix A - Sample Input File for the COPS Code

```
Simulation of 1-D Wave Propagation in AP
Max Cycle =   10000010 Max Time=   1.500e-06 nedit    =   02000000 iplot =  1 mtrls=  4
ntedt     =          0 njedt    =          7 nlayers  =          6 layfl  =        1
islide    =          0
jedit     =  850  910 1160  1203  1222  1240 1276
jmat      =    1    4    3     2     3     4
vproj     =  0.927e+05       angle         =      90.0
cl1       =      0.100 cq1      =       2.00 cl2      =       0.0 cq2      =      0.0
ism       =          0
dtmult    =       1.00
ncell  1  =        880 thick  1 =  1.270e+00    Sapphire
ncell  2  =        310 thick  2 =  3.041e-01         LiF
ncell  3  =          4 thick  3 =  1.000e-03       Epoxy
ncell  4  =         45 thick  4 =  3.000e-02          AP
ncell  5  =          4 thick  5 =  1.000e-03       Epoxy
ncell  6  =        600 thick  6 =  6.000e-01         LiF
SAPPHIRE               density  =      3.985 indp =  1 indd =  2 indc =  0
mu1       =  4.972e+12 mu2      =  4.972e+12 mu3    =  0.000e+00 Gamma/V=  2.420e+00
Yo        =  1.000e+30
G0        =  0.000e+12
AP                     density  =      1.954 indp =  1 indd =  2 indc =  0
mu1       =  1.273e+11 mu2      =  5.968e+11 mu3    =  1.030e+12 Gamma/V=  1.450e+00
Yo        =  2.600e+09
G0        =  15.05e+10
EPOXY                  density  =      1.184 indp =  1 indd =  2 indc =  0
mu1       =  1.037e+11 mu2      =  2.216e+10 mu3    =  4.931e+11 Gamma/V=  1.338e+00
Yo        =  5.000e+08
G0        =  2.593e+10
LIF                    density  =      2.641 indp =  1 indd =  2 indc =  0
mu1       =  7.013e+11 mu2      =  1.159e+12 mu3    =  9.480e+11 Gamma/V=  4.300e+00
Yo        =  1.000e+30
G0        =  0.000e+00
plots     =          5
vars      =    1    2    5   10   12
ifreq     =    3
```

References

1. *Handbook of Chemistry and Physics, 64th Edition*, CRC Press, Boca Raton, FL, 1983, p. B-67

2. G. Yuan, unpublished work at Shock Dynamics Center

3. Hall, A. R. and G. S. Pearson, *Oxid. and Comb. Rev.*, 3, 129 (1968)

4. Sandstrom, F. W., P. A. Persson, and B. Olinger, in *Ninth Symposium (International) on Detonation*, Office of Naval Research, Arlington, VA, 1989, p. 766

5. Choi, C. S., H. J. Prask, and E. Prince, *J. Chem. Phys.*, 61, 3523 (1974)

6. Sandusky, H. W., B. C. Glancy, D. W. Carlson, W. L. Elban, and R. W. Armstrong, *J. Prop. Power*, 7, 518 (1991)

7. Shoemaker, R. L., J. A. Stark, and R. E. Taylor, *High Temp.- High Press.*, 17, 429 (1985)

8. Brill, T. B., and F. Goetz, *J. Chem. Phys.*, 65, 1217 (1976)

9. Winey, J. M., Ph. D. Dissertation, Washington State University, 1995

10. Boteler, J. M. and Y. M. Gupta, Phys. Rev. Lett., 71, 3497 (1993)

Table 1: Physical Properties of Ammonium Perchlorate

Molecular Weight	117.5[a]
Density @ 298 K and 1 atm. (g/cc)	1.95[a]
Longitudinal Sound Velocity @ 1 atm. (km/s)	3.90[b]
Refractive Index @ 298 K and 1 atm.	1.482[a]
Orthorhombic-Cubic Transition Temperature @ 1 atm. (K)	513[c]
Specific Heat, c_v @ 298 K and 1 atm. (J/g-K)	1.26[d]
Gruneisen Parameter @ 298 K and 1 atm.	.74[d]

a) Value taken from Ref. 1.

b) Value taken from Ref. 2.

c) Value taken from Ref. 3.

d) Value calculated from data in Ref. 4.

Table 2: Summary of Experimental Results

Expt. Number	Experimental Configuration	Impact Configuration	Sample Thickness (mm)	Projectile Velocity (km/s)	Calc. Peak Pressure (GPa)	Calc. Peak Temperature (K)	Ringup Time (ns)
1 (96-003)	thick sample absorption	Sapp on AP/LiF	2.01	.828	5.9	375	single shock
2 (96-016)	thin sample absorption	Sapp on LiF/AP/LiF	.300	.927	11.0	440	177
3 (96-010)	thick sample Raman	Sapp on AP/LiF	3.64	.863	6.1	391	single shock
4 (96-022)	thin sample Raman	Sapp on LiF/AP/LiF	.377	.934	11.1	442	222
5 (96-033)	thin sample Raman	Sapp on LiF/AP/Sapp	.475	.861	15.8	446	304

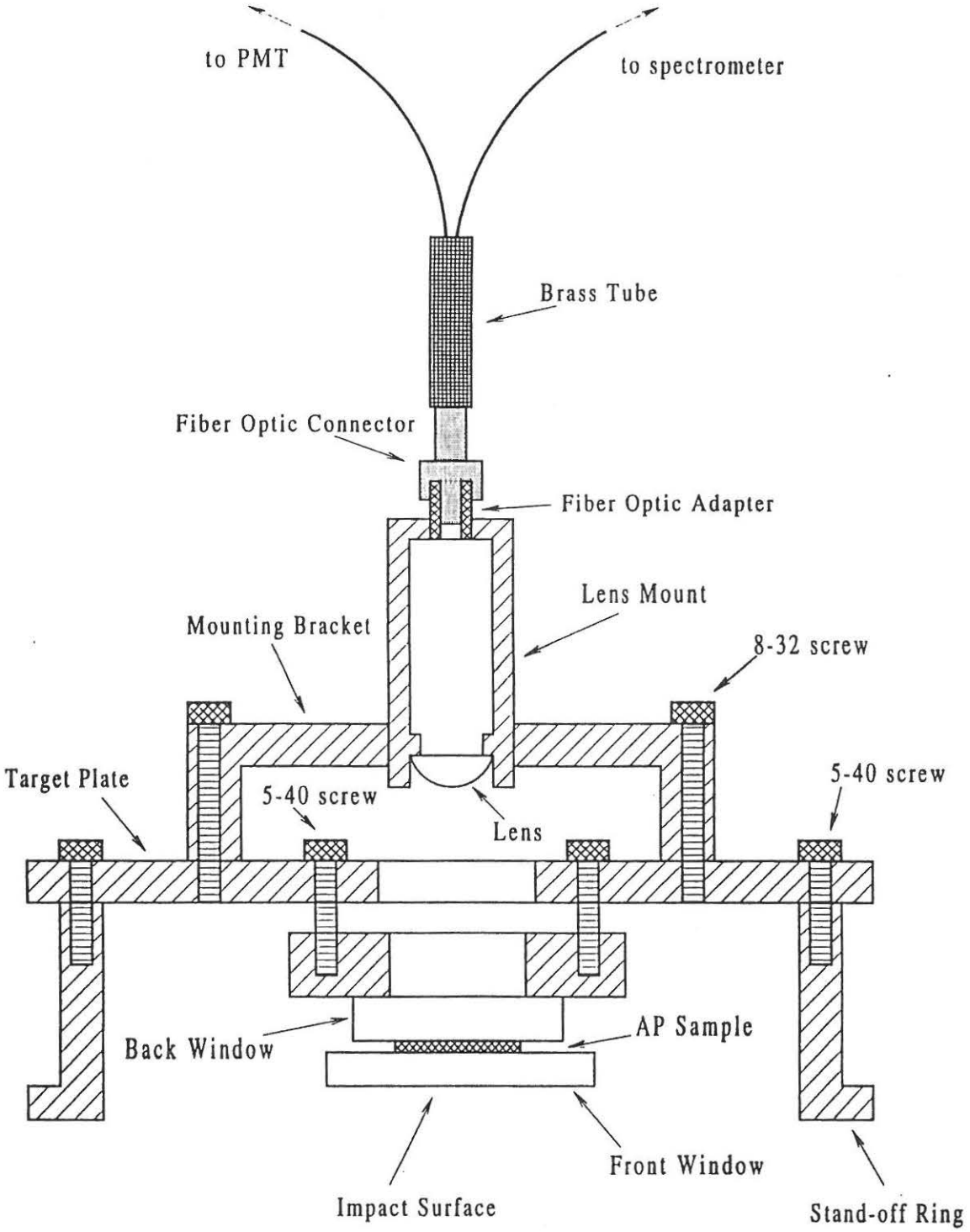

Figure 1 - Target Assembly - Experiment 2

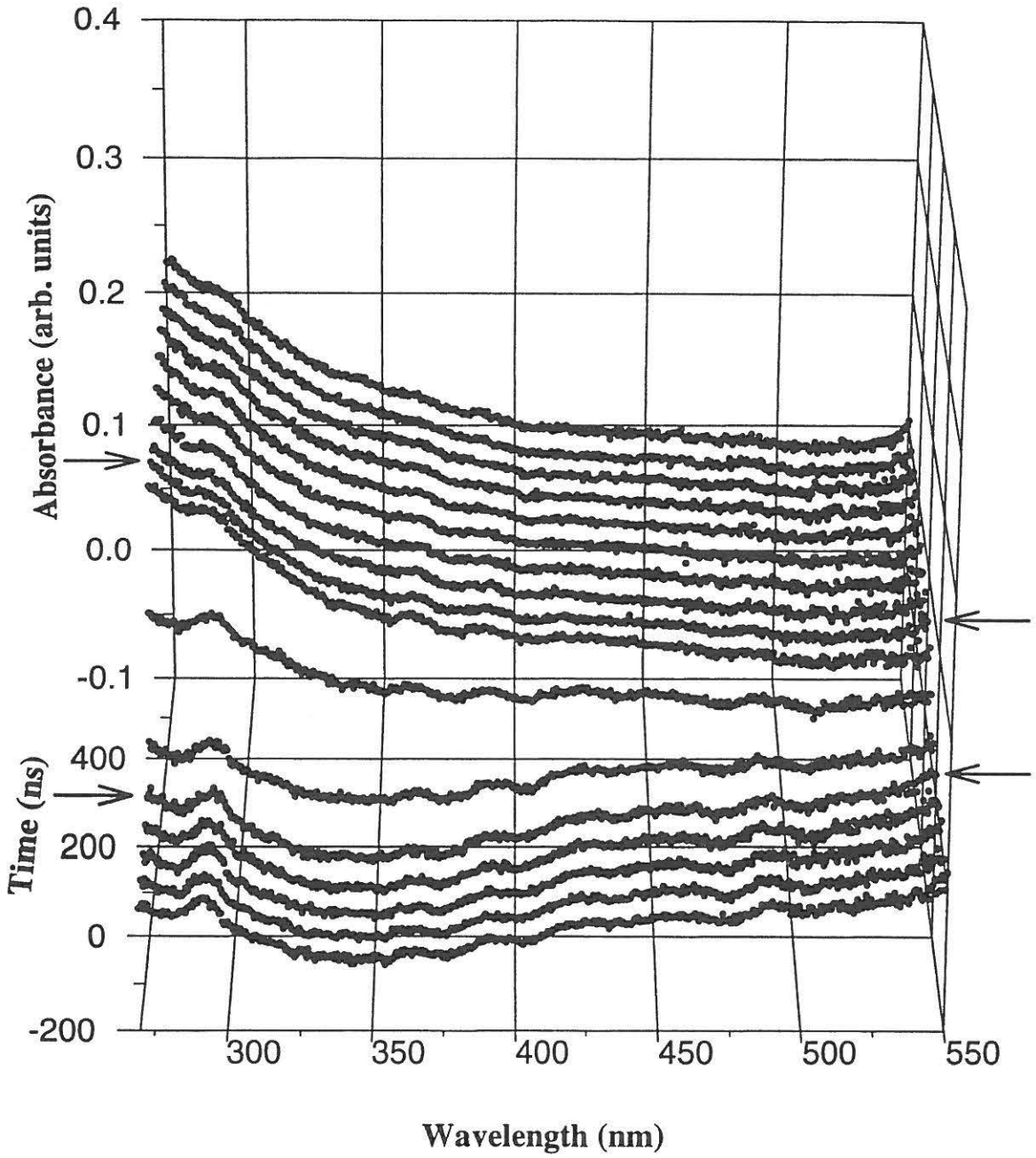

Figure 2 - Absorption Spectra of AP Shocked to 11.0 GPa (Exp. 2)
Time is relative to when the shock enters the sample. Time resolution is 50 ns. The two sets of arrows mark the times when the shock enters the sample and when peak pressure is reached.

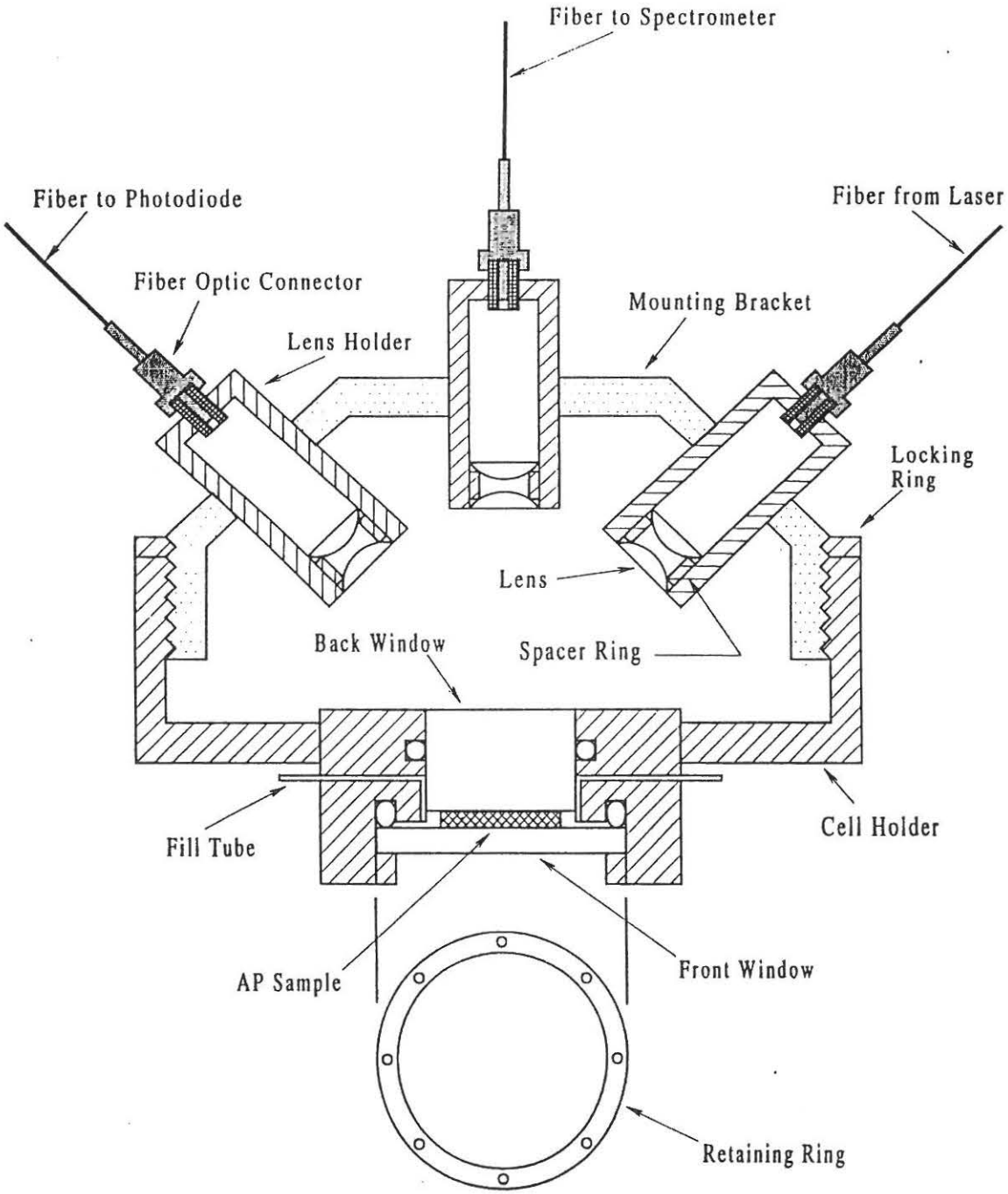

Figure 3 - Target Assembly - Experiment 5

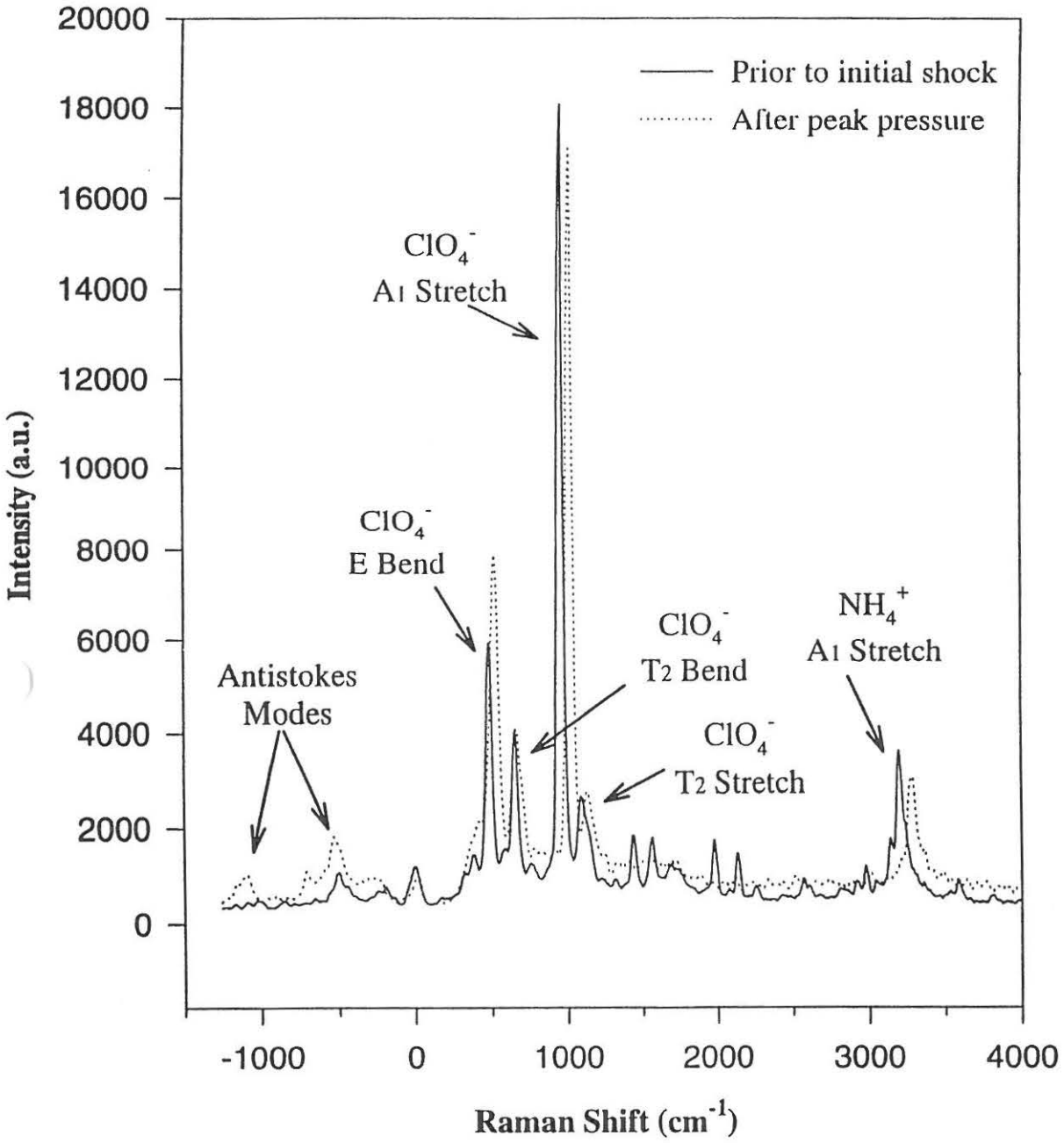

Figure 4 - Raman Spectra of AP Shocked to 15.8 GPa (Exp. 5)